

# Dust Formation in Primordial Type II Supernovae

Paolo Todini<sup>1</sup> and Andrea Ferrara<sup>2,3</sup>

<sup>1</sup> Università degli Studi di Firenze, Dipartimento di Astronomia, Largo Enrico Fermi 5, 50125 Firenze, Italy

<sup>2</sup> Osservatorio Astrofisico di Arcetri, Largo Enrico Fermi 5, 50125 Firenze, Italy

<sup>3</sup> Center for Computational Physics, University of Tsukuba, Tsukuba-shi, Ibaraki-ken, 305-8577, Japan

August 2000

## ABSTRACT

We have investigated the formation of dust in the ejecta of Type II supernovae (SNe), mostly of primordial composition, to answer the question of where are the first solid particles formed in the universe. However, we have also considered non-zero progenitor's metallicity values up to  $Z = Z_{\odot}$ . The calculations are based on standard nucleation theory and the scheme has been first tested on the well studied case of SN1987A, yielding results that are in agreement with the available data. We find that: *i*) the first dust grains are predominantly made of silicates, amorphous carbon (AC), magnetite, and corundum; *ii*) the largest grains are the AC ones, with sizes around  $300\text{\AA}$ , whereas other grain types have smaller radii, around  $10\text{--}20\text{\AA}$ . The grain size distribution depends somewhat on the thermodynamics of the ejecta expansion and variations in the results by a factor  $\approx 2$  might occur within reasonable estimates of the relevant parameters. Also, and for the same reason, the grain size distribution, is essentially unaffected by metallicity changes. The predictions on the amount of dust formed are very robust: for  $Z = 0$ , we find that SNe with masses in the range  $(12\text{--}35)M_{\odot}$  produce about  $0.08M_{\odot} \lesssim M_d \lesssim 0.3M_{\odot}$  of dust/SN. The above range increases by roughly 3 times as the metallicity is increased to solar values. We discuss the implications and the cosmological consequences of the results.

## 1 INTRODUCTION

Our understanding of galaxy formation is currently making tremendous advances and recent investigations have also focused on the formation of the first luminous sources (often referred to as PopIII objects). Several difficult questions arise when one deals with these peculiarly small collapsed objects (for a discussion see Ferrara 2000) primarily concerning the properties of their first stars and IMF (Tegmark *et al.* 1997, Abel *et al.* 1998, Bromm, Coppi & Larson 2000, Omukai & Nishi 1999, Susa & Umemura 2000, Nakamura & Umemura 2000, Ripamonti *et al.* 2000), their response to the energy injection of supernovae (SN) (MacLow & Ferrara 1999, Ciardi *et al.* 2000), their ability to form and preserve enough H<sub>2</sub> to provide the cooling for collapse (Ciardi, Ferrara & Abel 2000, Haiman, Abel & Rees 2000, Machacek, Bryan & Abel 2000), and their contribution to the reionization (Gnedin & Ostriker 1997, Gnedin 2000, Ciardi *et al.* 2000, Ciardi *et al.* 2000a) and metal enrichment (Ferrara, Pettini & Shchekinov 2000) of the IGM.

In spite of this flourishing activity little attention has been given to the role of dust in these early epochs. At lower redshifts the dramatic effects of dust have been appreciated when estimates of the cosmic star formation rate (SFR) were attempted via UV/visible surveys of distant galaxies. It was soon realized that approaches based on the “dropout” technique are poorly sensitive to dust-obscured galaxies. Hence, the SFR deduced in this way could represent a severe under-

estimate of the actual one, if even a rather modest amount of dust is present in the interstellar medium of the star forming galaxy. Also, some galaxies could be so heavily extinguished that they could be completely missed from the UV/visible census (Cimatti *et al.* 1997, Ferrara *et al.* 1999).

Direct indications of the existence of dust at high redshift come from the reddening of background quasars; indirect evidences of dust in damped Ly $\alpha$  systems have been obtained from the relative gas-phase abundances of Zn and Cr (Pettini *et al.* 1997). Fall *et al.* (1996) have calculated the cosmic infrared background from dust in damped Ly $\alpha$  systems, and found good agreement with FIR background deduced from COBE/FIRAS data, which also seem to imply the presence of dust. Recent detection of heavy elements, such as carbon and silicon (Lu *et al.* 1998, Cowie & Songaila 1998, Ellison *et al.* 2000) in very low column density Ly $\alpha$  clouds ( $\log N_{HI} < 14$ ) at redshift  $z \sim 3$  can potentially indicate that dust exists also in the Ly $\alpha$  forest: it is quite natural to assume that dust grains are associated with heavy elements. Dust in the forest clouds would be relevant to the understanding of their origin and association to PopIII objects, the heavy element enrichment pattern of intergalactic medium, and the thermal history of Ly $\alpha$  clouds (Ricotti & Gnedin 2000, Schaye *et al.* 2000).

The questions that we pose here are the following. When was dust first formed? Is grain formation possible starting from a metal-free environment? What are the dust prop-

erties and amount produced? How are these quantities affected by metallicity changes?

Dwek & Scalo (1980) have shown that dust injection in the ISM of the Galaxy from supernovae dominates other sources, if indeed grains can form and survive in the ejecta. This has become clear after the SN1987A event, in which dust has been unambiguously detected (Moseley *et al.* 1989, Kosaza, Hasegawa & Nomoto 1989). Indeed, the bulk of the refractory elements (characterized by higher melting temperatures, such as Si, Mg, Fe, Ca, Ti, Al etc.) is injected into the ISM by supernovae (McKee 1989). At high redshift, the contribution to dust production due to evolved stars (M and carbon stars, Wolf-Rayet stars, red giants and supergiants, novae) is even more negligible or absent. The reason is that the typical evolutionary timescale of these stars ( $\gtrsim 1$  Gyr) is longer than the age of the universe,  $t_H = 6.6h^{-1}(1+z)^{-3/2}$  Gyr in a EdS cosmology, if  $(1+z) \gtrsim 5$  (adopting  $h = 0.65$ ). Thus, it seems clear that if high redshift dust exists, it must have been produced by Type II SNe, to which we then devote the rest of this study.

## 2 DUST FORMATION MODEL

### 2.1 Dust nucleation and accretion

The formation of solid materials from the gas phase can occur only from a vapor in a supersaturated state. Because of the existence of a well defined condensation barrier, expressed by a corresponding "critical cluster" size, the formation of solid particles in a gaseous medium is described as a two-step process: *i*) the formation of critical clusters; *ii*) the growth of these clusters into macroscopic dust grains. The classical theory of nucleation (Feder *et al.* 1966, Abramham 1974) gives an expression for the nucleation current,  $J$ , *i.e.* the number of clusters of critical size formed per unit volume and unit time in the gas:

$$J = \alpha \Omega \left( \frac{2\sigma}{\pi m_1} \right)^{1/2} c_1^2 \exp \left\{ - \frac{4\mu^3}{27(\ln S)^2} \right\}, \quad (1)$$

where  $\mu = 4\pi a_o^2 \sigma / k_B T$  with  $a_o$  the radius of molecules (or atoms, depending on chemical species) in the condensed phase;  $\sigma$  is the specific surface energy (corresponding to surface tension in liquids),  $k_B$  is the Boltzmann constant and  $T$  the gas temperature;  $m_1$  and  $c_1$  are the mass and the concentration of the monomers in the gas phase, respectively;  $\Omega = (4/3)\pi a_o^3$  is the volume of the single molecules in the condensed phase,  $\alpha$  is the sticking coefficient and  $S$  the supersaturation ratio, defined below. The subsequent growth of the clusters occurs by accretion and is described by:

$$\frac{dr}{dt} = \alpha \Omega v_1 c_1(t), \quad (2)$$

with the condition:

$$r(0) = r_* = \frac{2\sigma \Omega}{k_B T \ln S}, \quad (3)$$

where  $v_1$  is the mean velocity of monomers,  $r(t)$  is the cluster radius at time  $t$ , and  $r_*$  is the cluster critical radius. Equations (1) and (2) describe nucleation and growth of solid particles in a gas composed of a single chemical species (*i.e.* reactions of the type  $Fe(gas) \rightarrow Fe(solid)$  or  $SiO(g) \rightarrow SiO(s)$ ). However, there are some compounds

(like forsterite,  $Mg_2SiO_4$ ) whose nominal molecule does not exist in the gas phase. These compounds form directly in the solid phase by means of a chemical reaction with the reactants in the gas phase. We need to extend the theory described above to this situation. Following Kozasa & Hasegawa (1987, see also Hasegawa & Kozasa 1988) we consider a vapor in a supersaturated state. In this vapor grains condense homologously via the reaction:

$$\sum_i \nu_i A_i = \text{solid compound}, \quad (4)$$

where  $A_i$ 's represent the chemical species of reactants and products in the gas phase and  $\nu_i$ 's are stoichiometric coefficients, which are positive for reactants and negative for products respectively. We make the following assumptions: *i*) the rates of nucleation and grain growth are controlled by a single chemical species, referred to as a key species. *ii*) the key species corresponds to the reactant with the least collisional frequency onto a target cluster. In this case, eqs. (1) and (2) become:

$$J = \alpha \Omega \left( \frac{2\sigma}{\pi m_{1k}} \right)^{1/2} c_{1k}^2 \exp \left\{ - \frac{4\mu^3}{27(\ln S)^2} \right\}, \quad (5)$$

and

$$\frac{dr}{dt} = \alpha \Omega v_{1k} c_{1k}(t), \quad (6)$$

where  $m_{1k}$ ,  $c_{1k}$  and  $v_{1k}$  are the mass, concentration and mean velocity of monomers of key species, respectively. In this case the supersaturation ratio is expressed by:

$$\ln S = - \frac{\Delta G_r}{RT} + \sum_i \nu_i \ln P_i, \quad (7)$$

where  $P_i$  is the partial pressure of the  $i$ -th specie,  $R$  is the gas constant and  $\Delta G_r$  is the Gibbs free energy for the reaction (4).

We investigate the formation of the following solid compounds:  $Al_2O_3$  (corundum), iron,  $Fe_3O_4$  (magnetite),  $MgSiO_3$  (enstatite),  $Mg_2SiO_4$  (forsterite) and amorphous carbon grains (ACG). These compounds are constituted by the most abundant heavy elements in the ejecta. Numerical constants used in our calculations are summarized in Tab. 1. The value of the sticking coefficient  $\alpha$  is set equal to 1 for all reactions; we have checked that the final results are insensitive to a different choice in the plausible range  $\alpha = 0.01 \div 1$ .

### 2.2 Supernova model

We now describe the adopted model for the SN ejecta. Before the explosion the progenitor develops the standard "onion skin" stratified structure, with a hydrogen-rich envelope, a helium layer, and several thinner heavy element layers up to a  $Fe - Ni$  core. During the explosion a shock wave propagates through the layers, reheats the gas and triggers the explosive nucleosynthesis phase. This phase lasts for few hours, then expansion cools the gas and the thermonuclear reactions turn off. After the explosion the SN starts to expand homologously, with velocity  $v \propto R$ , where  $R$  is the distance from the center. During the first weeks Rayleigh-Taylor instabilities cause the mixing of the internal layers (Fryxell, Müller & Arnett 1991). The early emergence of X-rays and

**Table 1.** Chemical reactions and numerical constants used in dust formation calculations.  
<sup>a</sup>Kozasa, Hasegawa & Nomoto 1989; <sup>b</sup>Kozasa *et al.* 1996; <sup>c</sup>Hasegawa & Kozasa 1988.

solid compound	chemical reaction	$\sigma$ [erg][cm] <sup>-2</sup>	$a_o$ [10 <sup>-8</sup> cm]
ACG	$C(g) \rightarrow C(s)$	1400 <sup>a</sup>	1.28
$Al_2O_3$	$2Al + 3O \rightarrow Al_2O_3$	690 <sup>a</sup>	1.72
$Fe$	$Fe(g) \rightarrow Fe(s)$	1800 <sup>c</sup>	1.41
$Fe_3O_4$	$3Fe + 4O \rightarrow Fe_3O_4$	410 <sup>a</sup>	1.80
$MgSiO_3$	$Mg + SiO + 2O \rightarrow MgSiO_3$	400 <sup>b</sup>	2.32
$Mg_2SiO_4$	$2Mg + SiO + 3O \rightarrow Mg_2SiO_4$	436 <sup>a</sup>	2.05

$\gamma$ -rays observed in SN 1987A (Itoh *et al.* 1987; Kumagai *et al.* 1988) can be explained if radioactive  $^{56}Co$  is mixed from the internal regions of the star into the external ones; more precisely, observations suggest mixing of the materials in the ejecta at least up to the outer edge of the helium layer. Dust grains are formed by heavy elements so we focus on the volume that containing them, *i.e.* the sphere of radius  $R$ , defined as the radius of the outer edge of the He-rich layer. It is thought that mixing forms clumps of heavy elements embedded in the He-rich layer. As a first approximation, we assume that mixing is complete, and that the gas has uniform density and temperature in the considered volume at any given time.

Photometric observations have shown that a SN emits typically  $10^{49}$  erg in electromagnetic energy, but current theoretical models predict kinetic energies  $E_{kin} \approx 10^{51}$  erg. The expansion velocity  $v$  is then given by:  $v \approx \sqrt{E_{kin}/M_{tot}}$ , where  $M_{tot}$  is the total mass ejected by the SN. We take the chemical composition of the expelled gas from the results of Woosley & Weaver 1995 (hereafter WW95), apart from the specific case of SN 1987A, see below. They determine the nucleosynthetic yields of isotopes lighter than A=66 (Zinc) for a grid of stellar masses and metallicities including stars in the mass range  $11 - 40 M_\odot$  and metallicities  $(Z/Z_\odot) = 0, 10^{-4}, 0.01, 0.1, 1$ . They also give the values for  $E_{kin}$  and  $M_{tot}$  for all the SN models considered. The range  $11 - 40 M_\odot$  is the most relevant mass range for the production of heavy elements. In fact, stars with mass between  $8$  and  $11 M_\odot$  are characterized by very thin heavy element layers, whereas stars heavier than  $40 M_\odot$  might be rare and give rise to a black hole partially swallowing the nucleosynthetic products (Maeder 1992).

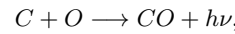
Expansion of the ejecta leads to cooling of the gas. We have already mentioned that the radiation losses are only a few percent of the total internal energy; their contribution to cooling is even smaller in the first week after the explosion due to the high opacity which prevents photons from escaping from the inner regions. Therefore, it is a good approximation to assume that the expansion is adiabatic, although this hypothesis becomes less correct in the advanced evolutionary stages. Radiation losses are also partly balanced by the heating provided by radioactive decay (especially of  $^{56}Ni \rightarrow ^{56}Co \rightarrow ^{56}Fe$ ). We neglect here these complications and assume that the expansion is adiabatic. In this case (for a perfect gas) the temperature evolution is given by

$$T = T_i \left( 1 + \frac{v}{R_i} t \right)^{3(1-\gamma)} ;$$

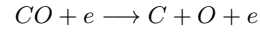
$\gamma$  is the adiabatic index,  $T_i$  and  $R_i$  are the temperature and the radius at the beginning of the computation,  $t$  is the time elapsed from this initial epoch. At the temperatures of interest ( $T < 6000$  K) the gas density is  $\approx 10^8$  atoms cm<sup>-3</sup> so the use of the perfect gas law is well justified. We set the values of  $R_i$ ,  $T_i$  and  $\gamma$  as follows. From photometric observations of SN 1987A (Catchpole *et al.* 1987) it is deduced that photosphere and the outer edge of He-rich layer overlap  $\approx 70$  days after the explosion, when the photospheric temperature is 5400 K and the radius  $R = 1.6 \times 10^{15}$  cm. For the adiabatic index we take  $\gamma = 1.25$  as in Kozasa, Hasegawa & Nomoto (1989). We generally use these fiducial values in our models, but we will consider the effects of varying the values of  $R_i$  and  $\gamma$  when discussing the results.

### 2.3 Molecule formation

In the ejecta of SN 1987A molecules of  $CO$  were detected for the first time in a SN (Meikle *et al.* 1989; Meikle *et al.* 1993; Bouchet & Danziger 1993) together with  $SiO$  (Aitken *et al.* 1988; Bouchet *et al.* 1991). These two molecules are very important for our study because carbon atoms bound in  $CO$  are not available to form ACG, whereas  $SiO$  molecules take part in the chemical path leading to the formation of  $MgSiO_3$  and  $Mg_2SiO_4$ . We investigate the process of molecule formation under the assumption of chemical equilibrium. In the absence of grains, molecular formation in the gas phase must have been initiated by radiative processes. We assume that formation of  $CO$  is dominated by radiative association (Lepp, Dalgarno & McCray 1990; Liu, Dalgarno & Lepp 1992):



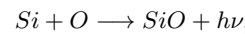
with a rate coefficient  $K_{ra}(CO)$ . The main destruction process of  $CO$  is the impact with the energetic electrons produced by the radioactive decay of  $^{56}Co$  (Liu & Dalgarno 1995):



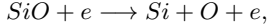
with a rate coefficient  $K_{rd}(CO)$ . In steady state, the abundance of  $CO$  is given by:

$$n(CO) = \frac{K_{ra}(CO)}{K_{rd}(CO)} n(C)n(O). \quad (8)$$

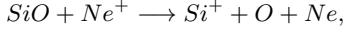
Analogously, radiative association is the most important mechanism for the formation of  $SiO$  (Liu & Dalgarno 1996) via the reaction:



with rate coefficient  $K_{ra}(SiO)$ . Silicon monoxide is mainly destroyed by impact with energetic electrons:



with rate coefficient  $K_{rd}(SiO)$  and by charge transfer with positive ions of  $Ne$  (Liu & Dalgarno 1996):



with rate coefficient  $K_{ct}(SiO)$ . The abundance of  $SiO$  is given by:

$$n(SiO) = \frac{K_{ra}(SiO)}{K_{rd}(SiO) + K_{ct}(SiO)n(Ne^+)} n(Si)n(O). \quad (9)$$

We assume for the rate coefficients the following values:

$$K_{ra}(CO) = 10^{-16} \times (-0.0398 + 1.25T_4 - 1.46T_4^2 + 0.88T_4^3 - 0.21T_4^4) \text{ cm}^3\text{s}^{-1},$$

(Gearhart, Wheeler & Swartz 1999, Dalgarno, Du & You 1990), where  $T_4 = T/10^4$  K.

$$K_{ra}(SiO) = 5.52 \times 10^{-18} T^{0.31} \text{ cm}^3\text{s}^{-1},$$

(Andreazza *et al.* 1995, Liu & Dalgarno 1996).

$$K_{ct}(SiO) = 2 \times 10^{-12} \text{ cm}^3\text{s}^{-1},$$

(Liu & Dalgarno 1996). The ejecta are only moderately ionized with fractional ionization  $\approx 10^{-2}$ ; hence, we assume  $n(Ne^+) = 0.02n(Ne)$ .

To calculate the rate coefficient  $K_{rd}(CO)$ , we assume the same rate of destruction by energetic electron impact for  $CO$  as for  $SiO$ , *i.e.*  $K_{rd}(CO) = K_{rd}(SiO)$ . High energy X-rays and  $\gamma$ -rays produced by the chain of radioactive decay  $^{56}_{28}Ni \rightarrow ^{56}_{27}Co \rightarrow ^{56}_{26}Fe$  interact by Compton scattering with the electrons in the ejecta. The average energy deposition rate per particle in the ejecta is (Woosley, Pinto & Hartmann 1989):

$$L_\gamma = 7.5 \times 10^{-8} \frac{N_i(^{56}Co)}{N_{tot}} \langle E_\gamma \rangle f_\gamma(K_{56}) \exp \left\{ -\frac{t}{\tau_{56}} \right\} \text{ MeV s}^{-1}.$$

$N_i(^{56}Co)$  is the total number of atoms of  $^{56}Co$  in the ejecta;  $N_{tot}$  is the total number of particles in the gas;  $\langle E_\gamma \rangle = 3.57$  MeV is the mean energy of  $\gamma$ -ray released by each decay;  $\tau_{56} = 111.26$  days is the e-folding time of  $^{56}Co$ . The deposition function,  $f_\gamma$  is proportional to the fraction of trapped  $\gamma$ -photons,

$$f_\gamma(K_{56}) = 1 - \exp \{-K_{56}\phi_o(t_o/t)\}^2,$$

with  $\phi_o = \phi(t_o)$ , the mass column density of the ejecta at some fiducial time  $t_o$ , and  $K_{56}$  an average opacity for  $^{56}Co$  decay  $\gamma$ -rays. We assume  $\phi_o = 7 \times 10^4 \text{ g cm}^{-2}$  at  $t_o = 10^6$  s and  $K_{56} = 0.033 \text{ cm}^2 \text{ g}^{-1}$ . These values are appropriate for SN 1987A but, lacking more detailed information, we extrapolate them to all our models. Finally, the estimated destruction rate of  $CO$  and  $SiO$  by energetic electron impact is

$$K_{rd}(CO) \equiv K_{rd}(SiO) = \frac{L_\gamma}{W_d} \text{ s}^{-1},$$

with  $W_d$  being the mean energy per dissociation, defined as the energy of primary electrons divided by the number of

molecule dissociations (Liu & Victor 1994). For a fractional ionization of the gas  $\approx 10^{-2}$ ,  $W_d = 152$  eV.

### 3 A TEST CASE: SN 1987A

To test and calibrate our dust formation model, we first apply it to SN 1987A, a case for which firm evidences of dust formation have been collected. In view of this test, we briefly summarize the relevant observational results.

#### 3.1 Observational results

The most relevant evidence of newly formed dust grains in the ejecta of SN 1987A is the blue shift of the line profiles. Spectroscopic observations detected this change between August 1988 and March 1989 (Lucy *et al.* 1989, Lucy *et al.* 1991). This effect is likely to be caused by the larger attenuation suffered by radiation received from receding matter due to dust grains distributed in the ejecta. The condensation efficiency, *i.e.* the dust mass expressed as a fraction of the maximum value permitted by the elemental abundances in the ejecta, derived by authors of observations from their data is  $\leq 10^{-3}$ . A further interesting observation is the stronger fading of the  $[SiI]\lambda 1.65\mu\text{m}$  line flux relative to the continuum after day 530. This can be interpreted as depletion of  $Si$  from the gas phase as a consequence of the formation of silicate grains. If the line fading is due solely to depletion, than the condensation efficiency rises to  $> 50\%$ .

Another evidence of the formation of dust is an IR continuum excess over that expected from a Planck spectrum fitted to the SN emission at optical wavelengths (Roche *et al.* 1989, Wooden *et al.* 1993). Dust grains extinguish UV-visible radiation from the central energy source, re-emitting in the IR bands. This process might be responsible for the observed increase in the 10 and  $20\mu\text{m}$  fluxes around day 350–450 (Roche *et al.* 1989, Bouchet & Danziger 1993, Meikle *et al.* 1993).

#### 3.2 Model Results

We now turn to the main results from our nucleation numerical computations obtained by solving the above equations. The chemical composition of the SN 1987A ejecta is taken from Nomoto *et al.* 1991. The value of expansion velocity of gas is set to  $v = 2100 \text{ km s}^{-1}$ . This is the minimum expansion velocity determined from the HI Pa absorption trough (McGregor 1988, Nulsen *et al.* 1990) and is thought to represent the expansion velocity of the inner edge of the hydrogen envelope. Fig. 1 shows the mass of dust formed in the ejecta as a function of the time elapsed since explosion for the different solid compounds found to be present. We note that there are two episodes of dust formation. In the first one, ACG (formation time  $t = 380$  days) and  $Al_2O_3$  ( $t = 430$  days) grains are formed. This process is likely to be responsible for the IR-excess observed at that time. In the second episode magnetite and silicate grains are formed, at about  $t = 600$  days. Two points are worth noticing to this concern. The first one is that this epoch corresponds to the formation of the predominant fraction of dust mass of the SN ( $0.57 M_\odot$  corresponding to about 84% of the total

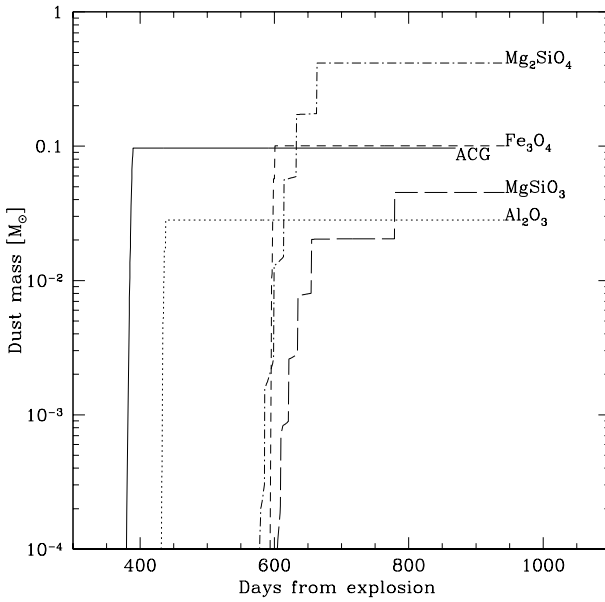


**Figure 1.** Dust formation as a function of time elapsed since explosion in SN1987A

amount); this dust formation episode might be responsible for the blueshift of line profiles, observed only after day 530, when ACG and  $Al_2O_3$  formed.

The second point is that the formation of  $MgSiO_3$  and  $Mg_2SiO_4$  might be related to the fading of the  $Si$  and  $Mg$  lines. The hypothesis that these elements form enstatite and forsterite would also be suggested by the behavior of the  $SiO$  molecule. The silicon monoxide rotovibrational line ( $v = 1 \rightarrow 0$ ,  $\lambda = 7.8\mu m$ ) emission was detected after 160 days (Aitken *et al.* 1988) and it remained clearly detectable until 519 days (Bouchet *et al.* 1991) but is no longer detected at 578 days (Roche *et al.* 1989). The time behavior of  $SiO$  emission can be understood by inspecting Fig. 2, where we show the predicted  $SiO$  mass vs. the observed mass as a function of time. Note the rapid fall at 660 days, 70 days after the beginning of silicate formation, probably due to the depletion of  $Si$  atoms; also our model seems to slightly overpredict (by a factor 3.1) the amount of  $SiO$  produced at early times. This could be due to our simplified treatment of the chemical network for this molecule or inaccuracies in the rate coefficients. The dust formation efficiency deduced here is 95%, consistent with that deduced from the  $Si$  line fading.

All together, we look at the above results as a satisfactory success of our model in reproducing, at least qualitatively, the principal features of dust formation in SN 1987A.

#### 4 DUST IN PRIMORDIAL SUPERNOVAE

In this Section we present the general results concerning dust formation in primordial SNe. We take the chemical compositions of the gas from Tables 16A and 16B of WW95, and the relevant results are reported in Tab. 2. There the chemical composition of the ejecta is given at  $2.5 \times 10^4$  s after the

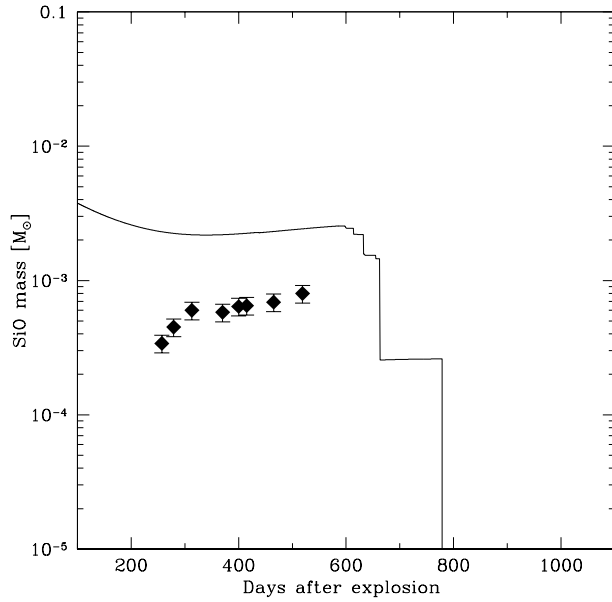


**Figure 2.** Evolution of the  $SiO$  mass (solid line) as a function of time compared with the observational data (points) taken from Liu & Dalgarno (1996).

explosion, when strong and electromagnetic reactions have ceased, but many nuclei have not yet decayed in their most stable form. Because dust formation occurs at 300–600 days after explosion, it is necessary to take into account the radioactive decay of such nuclei. In the SN models of WW95 the energy of explosion can be adjusted to give the desired kinetic energy of the ejecta, typically  $10^{51}$  erg. Following WW95, we explore the effects of  $E_{kin}$  variation by considering a low ( $E_{kin} = 1.2 \times 10^{51}$  erg, Case A) and a high ( $E_{kin} = 1.9 \times 10^{51}$  erg, Case B) value for this quantity. We discuss separately the two cases in the following.

#### 4.1 Low Kinetic Energy (Case A)

As the kinetic energy of the model is relatively low, this is not sufficient to completely expel the heavy elements external to the  $Ni - Fe$  core of the most massive SNe, and a variable amount of material falls back onto the core, probably forming a neutron star or a black hole. The fallback will mostly affect the inner layers, containing the heaviest elements; as a result, progenitors with masses larger than  $\approx 20M_\odot$  will be prevented from forming dust. For essentially the same reason, above  $M \approx 15M_\odot$ , only ACG grains are formed. Figs. 3–4 show the amount of dust formed as a function of progenitor mass, and the grain composition. ACG are typically the first solid particles to condense, depending on the models. The formation of these grains is quite fast with respect to the cooling time scale of the ejecta: most of the ACG dust mass forms in a narrow range of 30–40 K around  $T = 1800$  K. Subsequently, at a temperature of  $\approx 1600$  K  $Al_2O_3$  starts to condense, followed by  $Fe_3O_4$ ,  $MgSiO_3$  and  $Mg_2SiO_4$  at  $T \approx 1100$  K. Clearly this sequence is governed by the condensation temperature of a

**Table 2.** Adopted chemical composition of the supernova ejecta ( $2.5 \times 10^4$  s after explosion) for metallicity  $Z = 0$ . Data are taken from WW95 and corrected to take into account radioactive decay.

	$12M_{\odot}$	$13M_{\odot}$	$15M_{\odot}$	$18M_{\odot}$	$20M_{\odot}$	$22M_{\odot}$	$25AM_{\odot}$ $25BM_{\odot}$	$30AM_{\odot}$ $30BM_{\odot}$	$35AM_{\odot}$ $35BM_{\odot}$	$40AM_{\odot}$ $40BM_{\odot}$
<i>He</i>	4.08E+00	4.42E+00	4.90E+00	5.70E+00	6.32E+00	7.10E+00	7.33E+00 7.82E+00	9.11E+00 9.30E+00	8.17E+00 1.06E+01	8.63E+00 1.20E+01
<i>C</i>	4.30E-02	6.84E-02	1.45E-01	1.10E-01	8.98E-02	2.77E-01	8.31E-02 4.23E-01	1.09E-01 3.48E-01	1.25E-09 3.49E-01	7.73E-10 2.85E-01
<i>N</i>	5.41E-06	1.00E-05	2.46E-05	2.13E-06	1.76E-06	8.39E-05	2.39E-04 3.29E-04	3.64E-05 2.74E-03	2.13E-08 6.29E-05	2.66E-08 6.17E-06
<i>O</i>	6.67E-02	1.37E-01	4.00E-01	3.00E-02	9.21E-03	1.85E+00	9.67E-03 2.33E+00	2.65E-02 4.35E+00	3.08E-10 1.92E+00	4.19E-10 5.78E-01
<i>Ne</i>	2.61E-03	3.04E-02	9.28E-02	7.72E-04	2.12E-04	5.57E-01	5.79E-07 5.10E-01	4.66E-06 1.04E+00	1.37E-12 3.76E-01	1.95E-12 1.10E-02
<i>Na</i>	9.83E-06	1.90E-04	5.68E-04	9.57E-10	1.01E-09	3.90E-03	1.04E-08 2.85E-03	5.04E-08 3.88E-03	4.02E-13 1.86E-03	6.37E-13 1.07E-07
<i>Mg</i>	3.88E-03	1.50E-02	3.41E-02	4.80E-06	2.04E-06	9.52E-02	5.61E-08 9.38E-02	5.90E-07 2.49E-01	2.30E-13 4.83E-02	3.33E-13 2.89E-04
<i>Al</i>	7.19E-05	5.55E-04	1.31E-03	1.47E-10	1.09E-10	2.43E-03	8.73E-10 1.88E-03	1.18E-08 5.88E-03	9.62E-14 8.74E-04	1.43E-13 1.46E-08
<i>Si</i>	2.51E-02	3.41E-02	6.89E-02	2.79E-09	1.97E-09	1.66E-01	2.73E-09 2.32E-01	3.48E-08 1.24E-01	1.03E-09 1.77E-03	1.05E-10 2.89E-08
<i>S</i>	8.66E-03	1.35E-02	2.61E-02	1.18E-10	8.87E-11	1.09E-01	2.07E-09 1.06E-01	6.36E-08 4.59E-02	3.58E-13 2.82E-06	4.22E-13 4.32E-10
<i>Ca</i>	1.42E-03	3.01E-03	4.19E-03	8.57E-13	7.15E-13	2.38E-02	3.59E-10 1.75E-02	5.76E-09 8.78E-03	1.27E-26 2.06E-09	1.17E-17 5.71E-11
<i>Ti</i>	1.40E-04	1.71E-04	1.90E-04	3.27E-13	6.52E-14	3.25E-04	1.55E-10 3.47E-04	3.40E-09 4.80E-04	2.15E-26 1.79E-09	1.33E-26 1.42E-10
<i>Fe</i>	8.45E-02	2.00E-01	1.67E-01	4.93E-15	1.02E-17	1.74E-01	7.24E-11 2.99E-01	1.32E-09 3.35E-01	6.56E-36 5.36E-10	1.16E-35 7.01E-11
$^{56}Co$	8.15E-02	1.92E-01	1.62E-01	4.35E-20	3.03E-23	1.68E-01	2.14E-16 2.91E-01	3.69E-15 3.25E-01	8.19E-46 1.54E-15	9.29E-46 9.44E-16

given material. Also, the more refractory materials preferentially end up into larger grains: this is because an earlier formation can exploit a higher concentration of the key species favoring the accretion process. The typical size of ACG dust grains is  $a = 300$  Å, whereas  $Fe_3O_4$  grains have typically  $a = 20$  Å and  $Al_2O_3$ ,  $MgSiO_3$  and  $Mg_2SiO_4$  grains are even smaller ( $\approx 10$  Å). In spite of the high condensation temperature,  $Al_2O_3$  grains do not grow to sizes comparable to those of ACG, as their growth is limited by the low abundance of *Al*. In Figure 6 grain sizes of the most abundant compounds that form in supernova ejecta are shown for four values of  $Z$  (non zero metallicity cases are discussed later on). The two silicates (enstatite and forsterite) start to condense almost simultaneously; however,  $Mg_2SiO_4$  enters the supersaturation regime earlier than  $MgSiO_3$ . For this reason, forsterite grains grow quickly, strongly depleting the *Si* (or *Mg*) available. Figs. 3–4 clearly show that even starting from a primordial composition, early SNe can contribute a significant amount of dust: for Case A, about  $0.08M_{\odot} \lesssim M_d \lesssim 0.3M_{\odot}$  of dust/SN are produced. Intermediate mass progenitors are the most efficient sources, being able to convert up to 2% of their mass into solid particles. The reason is that they synthesize a considerable amount of heavy elements without suffering too much from the fallback process mentioned above.

## 4.2 High Kinetic Energy (Case B)

In this case the kinetic energy of the explosion for the progenitor masses 25, 30, 35 and  $40M_{\odot}$  is chosen equal to  $1.9 \times 10^{51}$  erg; for lower masses the energy of explosion is the same as in case A. This energy is sufficient to eject also the inner layers, which now can provide the elements to form grains of various chemical composition, *i.e.* not only ACG as in case A. In Fig. 5 we show the dust mass yield for Case B. Now SN up to masses  $\approx 35M_{\odot}$  are able to form dust. In addition, a SN of  $30M_{\odot}$  is able to produce about  $1.3M_{\odot}$  of dust (4.3% of its mass). The formation sequence and the grain size distribution are very similar to those discussed for Case A.

## 4.3 Effects of $R_i$ and $\gamma$ Variations

Up to now we have used the values of  $R_i$  and  $\gamma$  deduced from observations on SN 1987A. These values represent a reasonable approximation but they might well depend on the specific properties of the SN under examination. Therefore, as a sanity check, we investigate the dependence of our results on different choices for these parameters. As a benchmark, we focus on the  $M = 22M_{\odot}$  SN model (Case A) and increase or decrease the standard value of  $R_i = 1.6 \times 10^{15}$  cm by a factor 2.15; this corresponds to a variation of about 100 times in the initial volume of the ejecta. In Fig. 7 we compare the dust formation evolution and the final size of  $Fe_3O_4$  grains

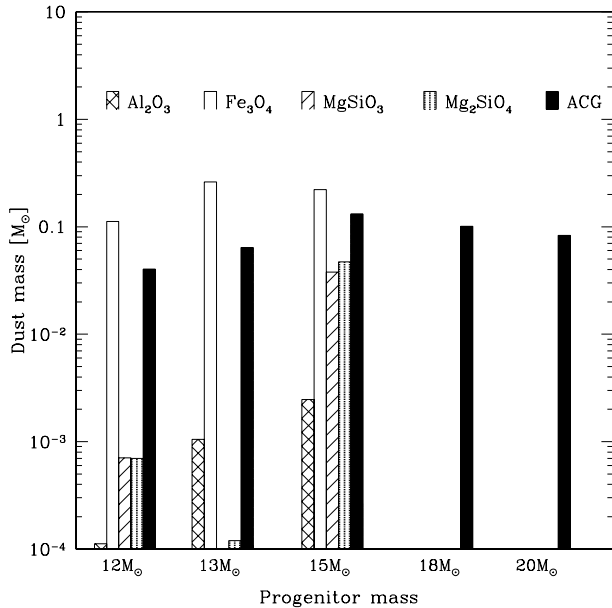


**Figure 3.** Dust mass formed as a function of the SN mass (in the range  $12M_{\odot} < M < 20M_{\odot}$ ) for initial metallicity  $Z = 0$  and kinetic energy of the explosion  $E_{kin} = 1.2 \times 10^{51}$  erg (Case A). Also shown is the grain composition.

for three values of  $R_i$ . The final masses of ACG,  $Al_2O_3$  and  $Fe_3O_4$  grains are almost unchanged in the three cases because the gas density remains high enough for the collisional time scale (regulating the formation/accretion processes) of these materials to remain shorter than the expansion one. However, the behavior of silicates depends on the choice of  $R_i$ . As a general rule,  $Mg_2SiO_4$  grains form first and grow faster than  $MgSiO_3$  ones, thus using up the condensable materials efficiently and ending up with a larger final total mass. However, for larger values of  $R_i$  (*i.e.* larger volume, lower gas density) this process is limited by the fact that the collisional scale becomes longer, thus stopping the accretion at earlier times. The grain size distribution shifts by about a factor 2 as  $R_i$  is varied by a factor (2.15). Thus the determination of the grain size distribution is relatively uncertain.

The adiabatic index  $\gamma$  gives a measure of the ability of the gas to cool:  $\gamma$  greater than the standard value of 1.25 cause the gas to reach the supersaturation state when the volume of the ejecta is smaller. Therefore, a larger  $\gamma$  case gives results similar to those obtained for the low  $R_i$  case discussed above. Figure 8 shows the dust formation evolution and final grain size distribution of  $Fe_3O_4$  grains for the  $M = 22M_{\odot}$  model (Case A) with  $\gamma = 1.4$ . The similarity with the previous case with  $R_i = 7.4 \times 10^{14}$  cm and  $\gamma = 1.25$  is evident. It has to be noted though that the variation range for  $\gamma$  (15%) is smaller than that for  $R_i$  (50%), which might indicate that the dust formation process is more sensitive to changes in the adiabatic index than in the initial radius.

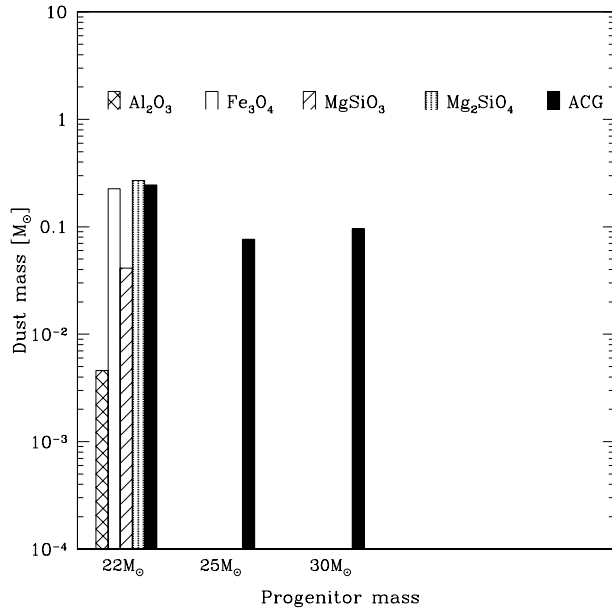


**Figure 4.** Same as Fig. 3, but for the SN mass range  $22M_{\odot} < M < 30M_{\odot}$ .

## 5 EXTENSION TO HIGHER METALLICITIES

We finally extend our results to non-primordial compositions by exploring the results for additional three metallicity values  $Z/Z_{\odot} = 10^{-4}, 10^{-2}, 1$ . The chemical composition for these models is also taken from WW95. We start by analyzing the dependence of the grain size distribution on metallicity. This is shown in the four panels of Fig. 6. Somewhat surprisingly, the dependence is almost absent, with grain radii ranging from 5 Å to 0.1  $\mu$ m for all values of  $Z$ . Also, the same material segregation is seen, with smaller grains being predominantly constituted by silicate and magnetite and the larger ones made by amorphous carbon. This behavior can be explained by the fact that the final grain size is governed by the thermodynamics of the ejecta expansion (and therefore sensitive to  $R_i$  and  $\gamma$ , as already pointed out before), but poorly affected by the ejecta composition.

The latter, instead, plays a more important role in determining the total amount of dust formed, as seen in Figs. 9–10 for Case A and Case B, respectively. Moving from  $Z = 0$  to higher metallicities we observe that a large number of SNe contribute to dust production: a clear example of this is the behavior of SNe with mass  $18\text{--}20 M_{\odot}$ , which increase their dust yield from  $< 0.1M_{\odot}$  up to  $0.5\text{--}0.6M_{\odot}$  for  $Z = 1$ . The enhancement of dust formation is due to the fact that the density of heavy elements in the ejecta becomes large enough to allow the state of supersaturation to be reached more easily. This trend results in a steady increase of the total amount of the dust produced in the four cases (obviously, when applying these results one has to weigh over the appropriate IMF); they are  $(2.06, 3.6, 4.5, 5.9) M_{\odot}$  for  $Z/Z_{\odot} = (0, 10^{-4}, 10^{-2}, 1)$ , respectively, for Case A. However, it is interesting to note that at each metallicity, the maximum amount of dust produced by a single SN varies little, and it is never higher than approximately  $1M_{\odot}$ . Fi-

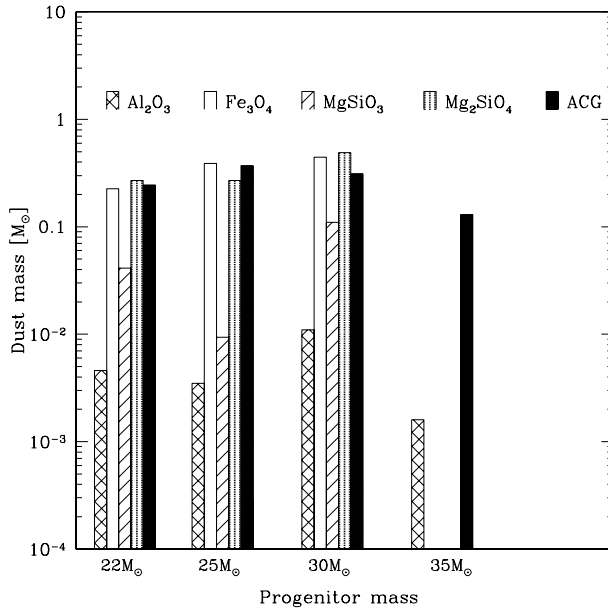


**Figure 5.** Same as in Fig. 3, but for kinetic energy of the explosion  $E_{kin} = 1.9 \times 10^{51}$  erg (Case B); the SN mass range is  $22M_{\odot} < M < 35M_{\odot}$ . For lower masses Case B gives the same results as Case A.

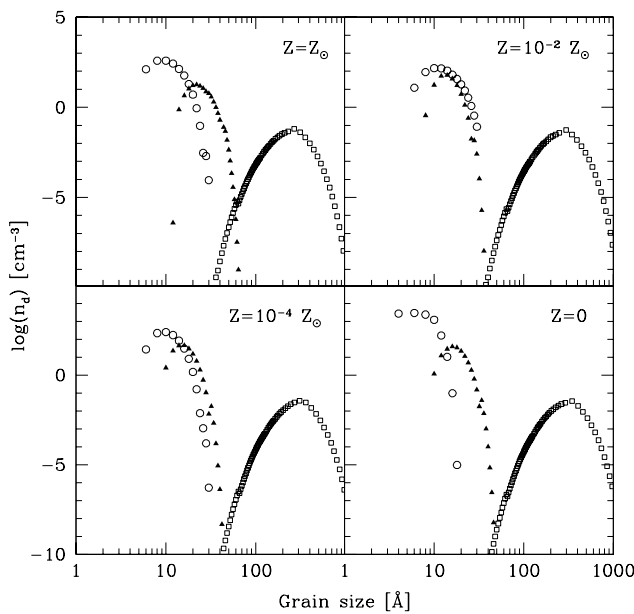


**Figure 6.** Grain size distribution of ACG (open squares),  $Fe_3O_4$  (solid triangles) and  $Mg_2SiO_4$  (open circles) grains for the  $M = 22M_{\odot}$  SN model; results are given for four different metallicities of the progenitor.

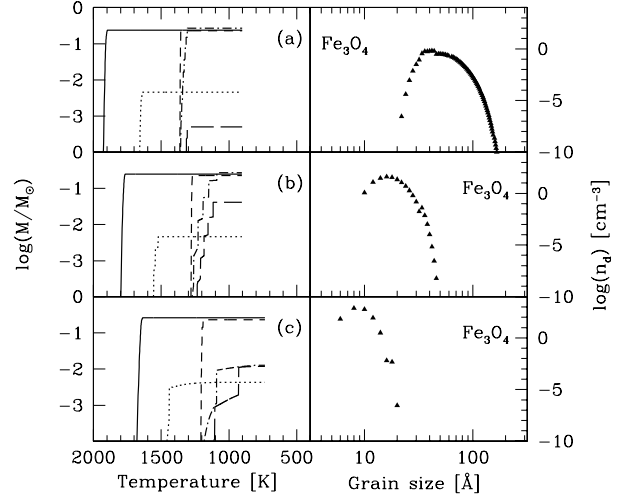


**Figure 7.** Dust formation (left, line types as in Fig. 1) and  $Fe_3O_4$  grain size distribution (right) for the  $M = 22M_{\odot}$  SN model; the three cases refer to different values of  $R_i$ : (a)  $7.5 \times 10^{14}$  cm, (b)  $1.6 \times 10^{15}$  cm (standard value), (c)  $3.4 \times 10^{15}$  cm.

nally, the differences between Casa A and Case B are found to be minor.

## 6 SUMMARY AND DISCUSSION

We have investigated the formation of dust in Type II supernovae mostly with primordial abundances, a property characterizing these events in the early universe; however, we have also considered non-zero metallicity values up to  $Z = Z_{\odot}$ . The calculations are based on standard nucleation theory and the scheme has been first tested on the well studied case of SN1987A, yielding results that are in satisfactory agreement with the available data (see Section 3). The main results of the paper are the following:

- The first solid particles in the universe are formed by Type II SNe. The dust grains are made of silicates (predominantly  $Mg_2SiO_4$ ), amorphous carbon (ACG), magnetite ( $Fe_3O_4$ ), and corundum ( $Al_2O_3$ ) and form about 300-660 days after explosion.
- The largest grains are the ACG, with sizes around 300 Å, whereas other grain types have smaller radii, around 10-20 Å. The grain size distribution depends considerably on the thermodynamics of the ejecta expansion (characterized by their initial radius and adiabatic index) and variations in the results by a factor  $\approx 2$  might occur within the estimated range of  $R_i$  and  $\gamma$ . Also, and for the same reason, the grain size distribution, is essentially unaffected by metallicity changes.
- The amount of dust formed is instead very robust to variations in  $R_i$  and  $\gamma$ . For  $Z = 0$ , we find that SN with masses in the range  $(12-35)M_{\odot}$  produce about

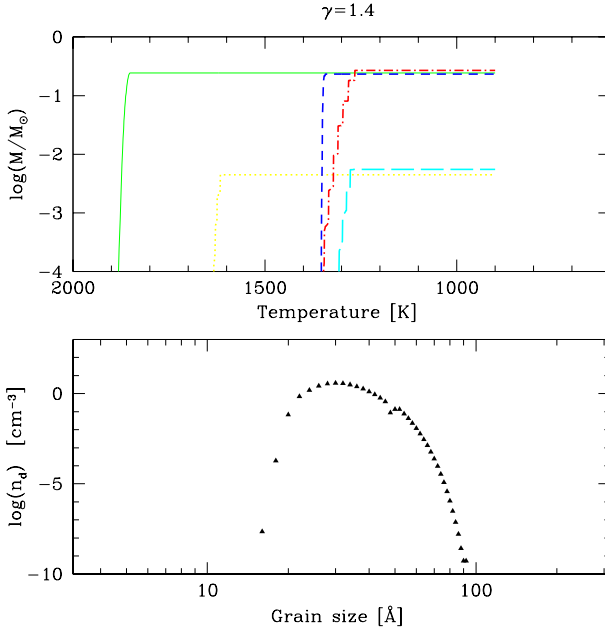


**Figure 8.** Dust formation (top) and  $Fe_3O_4$  grain size distribution (bottom) for the  $M = 22M_\odot$  SN with  $\gamma = 1.4$ .

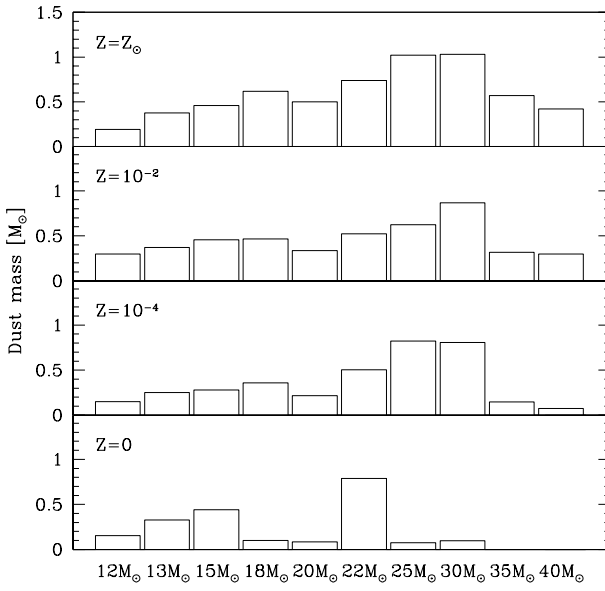


**Figure 9.** Total dust mass produced as a function of SN mass and different metallicity of the progenitor (Case A).

$0.08M_\odot \lesssim M_d \lesssim 0.3M_\odot$  of dust/SN in the low kinetic energy explosion case; slightly higher final yields are obtained in the high kinetic energy case. The above range increases by roughly 3 times as the metallicity is increased to solar values.

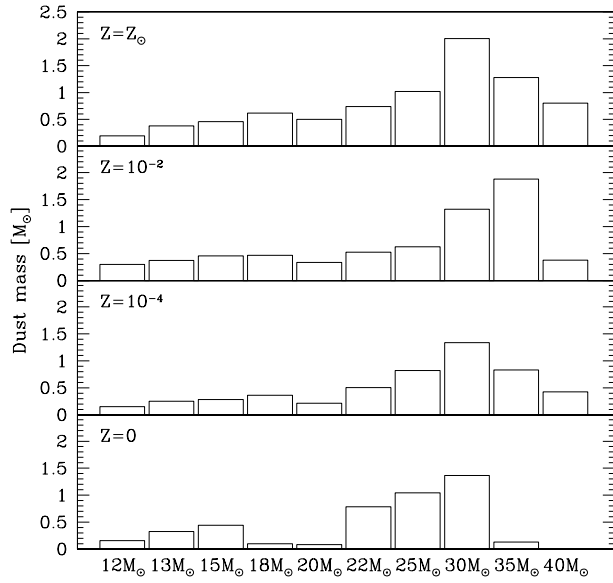


**Figure 10.** Same of Figure 9, but for Case B.

The previous results clearly show that it is likely that dust has been present in the universe immediately after the first stars appeared. This has a large number of consequences that it will be necessary to study in detail. Among possible effects, the most outstanding ones concern the opacity of the universe at high  $z$ , spectral distortions in the Cosmic Microwave Radiation caused by dust re-emission of absorbed UV-optical light, catalyzation of  $H_2$  molecular hydrogen formation and heavy elements depletion in the interstellar medium of pristine galaxies and in the intergalactic medium.

The first two issued were already discussed in detail by Loeb & Haiman (1997) and Ferrara *et al.* (1999), and we defer the interested readers to those works for details. In short, the expected IGM opacity contributed by dust around the observed wavelength  $\lambda \sim 1\mu m$  is  $\sim 0.13$  and it rapidly increases to  $\approx 0.35$  at  $z = 20$ . The expected CMB spectral distortions due to high- $z$  dust is only  $\sim 1.25 - 10$  times smaller than the current COBE upper limit, but these numbers might depend crucially on the formation epoch and abundance of dust.

In addition to the above effects, Type II SNe can also initiate molecular hydrogen formation on dust grain surfaces rather than in the gas phase, the second process being the only viable in a dust free environment. As already mentioned, at high redshift Type II SNe are the only possible sources of dust, due to the short age of the universe and the long evolutionary timescales characterizing more conventional dust sources, as for example evolved stars. Thanks to the above results we can now answer the following question: what is the minimum amount of dust required in order for the molecular hydrogen formation on grains to become competitive with the gas phase one? An order-of-magnitude answer can be obtained by comparing the two formation rates. At the low densities relevant here,  $H_2$  is formed in the

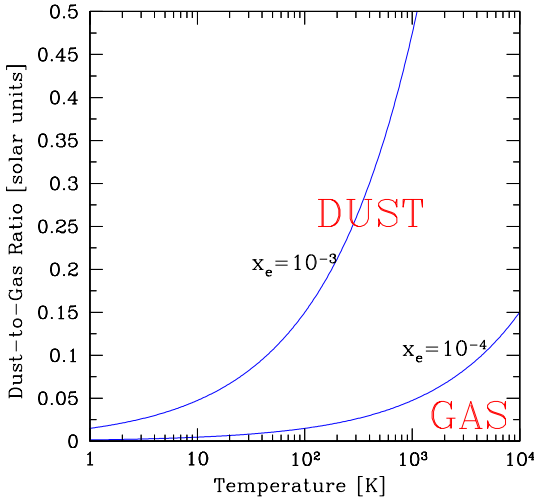


**Figure 11.** Comparison between molecular hydrogen formation rates in the gas phase and on dust grain surfaces as a function of the dust-to-gas ratio and gas temperature. Above the two curves, indicating the equality between the rates for two different values of the electron fraction  $x_e = 10^{-3} - 10^{-4}$ ,  $H_2$  formation on grains dominates.

gas phase mainly via the channel  $H + e^- \rightarrow H^- + h\nu$ , at rate  $k_8$  (the rate coefficient  $k_8$  is given in Abel *et al.* 1997); formation via the  $H_2^+$  channel, when included, is found to be negligible in our case. Therefore the formation rate in the gas phase is  $\mathcal{R} \simeq k_8 n_{H^-} n_H$ . The formation rate on grain surfaces is instead given by  $\mathcal{R}_d \simeq 0.5 \langle \gamma c_s \sigma \rangle n_d n_H$ , where  $\gamma$  is the sticking coefficient,  $c_s$  is the sound speed in the gas, and  $\sigma$  is the grain cross section. The equality between the two rates can be cast into the following form:  $\mathcal{D} = 0.1 \sqrt{T} x_e$ , where  $\mathcal{D}$  is the dust-to-gas ratio normalized to its Galactic value,  $T$  is the gas temperature and  $x_e$  the gas ionization fraction. For typical parameters of the PopIII objects (Ciardi *et al.* 2000),  $H_2$  production on dust grains becomes dominant once  $\mathcal{D}$  is larger than 5% of the local value. With the dust yields calculated above, we then conclude that only about 50 SN are required to enrich in dust to this level a primordial object. Clearly, early dust formation might play a role in the formation of the first generation of objects.

Even in larger galaxies, which will form later on when the overall metallicity and dust levels in the universe have increased, dust will be at least as important. For example, on the scale of the molecular clouds in a galaxy, it will provide the opacity to stop the infall on forming protostars, hence possibly changing the properties of the IMF, and to allow the cloud to self-shield from damaging  $H_2$  photodissociating UV radiation. Finally, dust photoelectric heating is known to be the major heating source for the diffuse ISM, and hence participating to the onset of its observed multi-phase structure (Ricotti, Ferrara & Miniati 1997, Spaans & Norman 1997).

The fate of the dust that we predict from Type II SNe has yet to be determined. What fraction of the grains will be able to survive the passage through the reverse shocks at which the ejecta are thermalized? Grains in a hot gas are essentially destroyed via thermal sputtering, *i.e.* collisions with ions or electrons with Maxwellian velocity distribution. However, in spite of the still poorly understood underlying physics, it seems unlikely that the efficiency of grain destruction in an adiabatic shock can be higher than 10% (McKee 1989). Grains are more likely to be destroyed behind radiative shocks, by the combined effects of a greatly enhanced gas density and betatron acceleration that increases the grain Larmor frequency. However, if, as expected, the magnetic field is weak at high  $z$ , the efficiency cannot be very high. The grains then will follow the fate of the gas and will likely be expelled in the IGM, as PopIII object suffer complete blowaway of their gas (Ciardi *et al.* 2000). Once in the intergalactic space, dust might have strong influence, for example, on the determination of cosmological parameters via the observation of high  $z$  (Type I) SN (Aguirre 1999, Croft *et al.* 2000).

As a final remark, we have seen that SNe with mass above  $M = 15M_\odot$  predominantly form amorphous carbon grains (the ejecta of these stars have higher C/O ratios); in doing so, they use up virtually all the available carbon yield in the ejecta. This implies that carbon in the IGM at high redshift will be strongly depleted above redshifts at which only Type II SNe contribute to the metal enrichment of the universe. It will be then possible to test this prediction once a sample of target sources at  $z \gtrsim 5$  will become available for absorption line studies.

This work was completed as one of us (AF) was a Visiting Professor at the Center for Computational Physics, Tsukuba University, whose support is gratefully acknowledged.

## REFERENCES

Abel, T., Anninos, P., Norman, M. L. & Zhang, Y. 1998, ApJ, **508**, 518  
 Abel, T., Anninos, P., Zhang, Y. & Norman, M. L. 1997, NewA, **2**, 181  
 Aguirre, A. 1999, ApJ, **533**, 1  
 Aitken D.K., Smith C.H., James S.D., Roche P.F., Hyland A.R. & McGregor P.J., 1988, MNRAS, **231**, 7P  
 Andreazza C.M., Singh P.D. & Sanzovo G.C., 1995, ApJ, **451**, 889  
 A. Ferrara, S. Bianchi, A. Cimatti & C. Giovanardi 1999, ApJSS, **123**, 437  
 Bouchet P. & Danziger I.J., 1993, A. & A., **273**, 451  
 Bouchet P. Danziger I.J. & Lucy L.B., 1991, *Supernovae*, ed. S.E. Woosley, Springer-Verlag, New York p.49  
 Bromm, V., Coppi, P. S. & Larson, R. B. 1999, ApJ, **527**, 5  
 Catchpole *et al.*, 1987, MNRAS, **229**, 15P  
 Ciardi, B., Ferrara, A., Governato, F. & Jenkins, A. 2000, MNRAS, **314**, 611  
 Ciardi, B., Ferrara, A., & Abel, T. 2000, ApJ, **533**, 594  
 Ciardi, B., Ferrara, A., Marri, S. & Raimondo, G. 2000a, preprint (astro-ph/0005181)  
 Cimatti, A., Bianchi, S., Ferrara, A., & Giovanardi, C. 1997, MNRAS, **290**, L43

Cowie, L.L. & Songaila, A., 1998, *Nature*, **394**, 44

Croft, R. A. C., Davé, R., Hernquist, L. & Katz, N. 2000, *ApJ*, **534**, 123

Dalgarno A., Du M.L. & You H., 1990, *ApJ*, **349**, 675

Dwek, E. & Scalo, J. M. 1980, *ApJ*, **239**, 193

Ellison, S. L., Lewis, G. F., Pettini, M., Chaffee, F. H. & Irwin, M. J., 1999, *ApJ*, **520**, 456

Fall, S. M., Charlot, S. & Pei, Y. C. 1996, *ApJ*, **464**, L43

Feder J., Russel K.C., Lothe J. & Pound J.M., 1966, *Adv. in Phys.*, **15**, 111

Ferrara A., Nath B., Sethi S.K. & Shchekinov Y., 1999, *MNRAS*, **303**, 301

Ferrara, A., Pettini, M. & Shchekinov, Y. 2000, preprint (astro-ph/0004349)

Ferrara A. 2000, *The Physics of Galaxy Formation*, H. Susa *et al.* eds., preprint (astro-ph/0007179)

Fryxell B., Müller E. & Arnett D., 1991, *ApJ*, **367**, 619

Gearhart R.A., Wheeler J.C. & Swartz D.A., 1999, *ApJ*, **510**, 944

Gnedin, N. Y., & Ostriker, J. P., 1997, *ApJ*, **486**, 581

Gnedin, N. Y. 2000, *ApJ*, **535**, 530

Haiman, Z., Abel, T. & Rees, M. J., 2000, *ApJ*, **534**, 11

Hasegawa H., & Kozasa T., 1988, *Prog. Theor. Phys. Supp.*, **96**, 107

Itoh M., Kumagai S., Shigeyama T., Nomoto K. & Nishimura J., 1987, *Nature*, **330**, 233

Kozasa T. & Hasegawa H., 1987, *Prog. Theor. Phys.*, **77**, 1402

Kozasa T., Hasegawa H. & Nomoto K., 1989, *ApJ*, **344**, 325

Kozasa T., Dorschner J., Henning T. & Stognienko R., 1996, *A. & A.*, **307**, 551

Kumagai S., Itoh M., Shigeyama T., Nomoto K. & Nishimura J., 1988, *A. & A.*, **197**, L7

Lepp S., Dalgarno A. & McCray R., 1990, *ApJ*, **358**, 262

Liu W. & Victor G.A., 1994, *ApJ*, **435**, 909

Liu W. & Dalgarno A., 1995, *ApJ*, **454**, 472

Liu W. & Dalgarno A., 1996, *ApJ*, **471**, 480

Liu W., Dalgarno A. & Lepp S., 1992, *ApJ*, **396**, 679

Loeb A. & Haiman Z., 1997, *ApJ*, **490**, 571

Lu, L., Sargent, W. L. W., Barlow, T.A., & Rauch, M. 1998, *ApJ*, submitted (astro-ph/9802189)

Lucy L.B., Danziger I.J., Gouiffes C. & Bouchet P., 1989, *Structure and dynamics of the interstellar medium*, Proceedings of IUA Colloquium No. 120, ed. Tenorio-Tagle G., Moles M., Melenick J.

Lucy L.B., Danziger I.J., Gouiffes C. & Bouchet P., 1991, *Supernovae*, The tenth Santa Cruz workshop in astronomy and astrophysics, ed. Woosley S.

MacLow, M.-M. & Ferrara, A. 1999, *ApJ*, **513**, 142

Machacek, M. E., Bryan, G. L. & Abel, T. 2000, preprint (astro-ph/0007198)

Maeder A., 1992, *A&A*, **264**, 105

McGregor P.J., 1988, *Proc. Astr. Soc. Australia*, **7**, 450

McKee, C. F. 1989, in *Interstellar Dust*, IAU Symp. 135, eds. L. J. Allamandola & A. G. G. M. Tielens, (Kluwer: Dordrecht), 431

Meikle W.P.S., Allen D.A., Spyromilio J. & Varani G.-F., 1989, *MNRAS*, **238**, 193

Meikle W.P.S., Spyromilio J., Allen D.A., Varani G.-F. & Cumming R.J., 1993, *MNRAS*, **261**, 535

Moseley, S. H., Dwek, E., Glaccum, W., Graham, J. R., & Loewenstein, R. F. 1989, *Nature*, **340**, 697

Nakamura, T. & Umemura, M. 2000, preprint

Nomoto, K., Shigeyama, T., Kumagai, S. & Yamaoka, H. 1991, *Supernovae*, ed. S.E. Woosley, Springer-Verlag, New York p. 176

Nulsen P.E.J., Wood P.R., Gillingham P.R., Bessell M.S., Dopita M.A. & McCowage C., 1990, *ApJ*, **358**, 266

Omukai, K. & Nishi, R. 1999, *ApJ*, **518**, 64

Pettini, M., King, D. L., Smith, L. J. & Hunstead, R. W. 1997, *ApJ*, **478**, 536

Ricotti, M., Gnedin, N. & Shull, J. M. 2000, *ApJ*, **534**, 41

Ricotti, M., Ferrara, A. & Miniati, F. 1997, *ApJ*, 485, 254

Ripamonti, E., Haardt, F., Colpi, M. & Ferrara, A. 2000, in preparation

Roche P.F., Aitken D.K., Smith S.D. & James S.D., 1989, *Nature*, **337**, 533

Schaye, J., Theuns, T., Leonard, A. & Efstathiou, G., 2000, *MNRAS*, **315**, 600

Spaans, M. & Norman, C. A. 1997, *ApJ*, **483**, 87

Susa, H. & Umemura, M. 2000, *ApJ*, **537**, 578

Tegmark M., Silk J., Rees M., Blanchard A., Abel T. & Palla F., 1997, *ApJ*, **474**, 1

Wooden D.H., Rank D.M., Choen M., Pinto P.A. & Axelrod T.S., 1993, *ApJS*, **88**, 477

Woosley S.E., Pinto P.A. & Hartmann D., 1989, *ApJ*, **346**, 395

Woosley S.E. & Weaver T.A., 1995, *ApJS*, **101**, 181 (WW95)